The orphan nuclear receptor NR4A3 controls the differentiation of monocyte-derived dendritic cells following microbial stimulation

Salix Boulet[a], Jean-François Daudelin[a], Livia Odagiu[a,b], Adam-Nicolas Pelletier[a,b], Tae Jin Yun[c,d], Sylvie Lesage[a,b], Cheolho Cheong[b,c,d], and Nathalie Labrecque[a,b,e,1]

[a]Laboratory of Immunology, Maisonneuve-Rosemont Hospital Research Center, Montreal, QC H1T 2M4, Canada; [b]Département de Microbiologie, Infectiologie, et Immunologie, Université de Montréal, Montréal, QC H3C 3J7, Canada; [c]Laboratory of Cellular Physiology and Immunology, Institut de Recherches Cliniques de Montréal, Montréal, QC H2W 1R7, Canada; [d]Division of Experimental Medicine, Department of Medicine, McGill University, Montreal, QC H3A 1A3, Canada; and [e]Département de Médecine, Université de Montréal, Montréal, QC H3C 3J7, Canada

Edited by Kenneth M. Murphy, Washington University School of Medicine in St. Louis, St. Louis, MO, and approved June 12, 2019 (received for review December 14, 2018)

In response to microbial stimulation, monocytes can differentiate into macrophages or monocyte-derived dendritic cells (MoDCs) but the molecular requirements guiding these possible fates are poorly understood. In addition, the physiological importance of MoDCs in the host cellular and immune responses to microbes remains elusive. Here, we demonstrate that the nuclear orphan receptor NR4A3 is required for the proper differentiation of MoDCs but not for other types of DCs. Indeed, the generation of DC-SIGN$^+$ MoDCs in response to LPS was severely impaired in *Nr4a3*$^{-/-}$ mice, which resulted in the inability to mount optimal CD8$^+$ T cell responses to gram-negative bacteria. Transcriptomic analyses revealed that NR4A3 is required to skew monocyte differentiation toward MoDCs, at the expense of macrophages, and allows the acquisition of migratory characteristics required for MoDC function. Altogether, our data identify that the NR4A3 transcription factor is required to guide the fate of monocytes toward MoDCs.

nuclear receptors | NR4A3 | monocyte-derived dendritic cells | LPS response

Dendritic cells (DCs) play crucial roles in the induction of the adaptive immune response of T cells to pathogens. Their ability to sense microbial molecular patterns using innate receptors and to display peptidic fragments of microbes on MHC class I and II (MHCI and MHCII) molecules allows them to act as extremely efficient antigen-presenting cells to prime naive T cell responses. Given the central role of DCs in linking the innate and adaptive immune responses, substantial efforts were made in studying the ontology and function of different DC subsets to better exploit their roles in infectious diseases. Currently, DCs are broadly categorized into two main groups: conventional DCs (cDCs) and plasmacytoid DCs (pDCs). Both cDCs and pDCs originate in the bone marrow (BM) from a macrophage/dendritic cell progenitor (MDP) that can further differentiate into the common DC progenitor (CDP). This progenitor can mature into a pDC, which requires the transcription factor E2-2 (1), or specify into precommitted progenitors (pre-DCs) that give rise to cDCs (2). Based on the requirement for lineage-defining transcription factor for their development and function, cDCs can be subdivided into two main subsets (reviewed in ref. 3). cDC1 requires IRF8, BATF3, NFIL3, ID2, and BCL6 for its development, whereas cDC2, which expresses IRF4, is heterogeneous and comprises both NOTCH2- and KLF4-dependent populations. Understanding the transcriptional networks controlling the generation of DC subsets has facilitated the engineering of mouse models in which a specific cDC type is depleted, making it possible to define the unique functions of each cDC subset in the immune response. For example, the use of *Batf3*$^{-/-}$ mice has revealed the biological importance of IRF8$^+$ cDC1 cells in cross-priming and in the generation of resident memory T cells (4, 5). Within the IRF4$^+$ cDC2 subset, NOTCH2-dependent DCs were shown to be crucial for early innate protection to *Citrobacter rodentium* infection (6).

In addition to cDCs and pDCs, monocyte-derived DCs (MoDCs) have been described (7–11). In response to several types of microbial stimulation, monocytes differentiate into MoDCs; they upregulate CD11c and MHCII, present antigen, and modulate the T cell response. For example, upon LPS exposure, monocytes convert into DC-SIGN$^+$ MoDCs, which also express CD206, CD14, and Sirpα (7). They locate to the T cell zone of the skin-draining lymph nodes (skLNs) and exhibit efficient T cell priming and cross-priming in vitro. However, the in vivo role and the transcriptional requirements for the differentiation of these MoDCs has yet to be demonstrated.

The transcriptional requirements for the differentiation of monocytes into MoDCs have not been as extensively studied as that of the development of cDCs. This is due, in part, to the difficulty in distinguishing MoDCs from both macrophages and other cDC subsets, especially in inflammatory conditions. The identification of the transcription factor ZBTB46 and the C-type lectin receptor DNGR-1 (encoded by *Clec9a*) as genetic tracers of DC lineages has helped clarify some of the issues associated with inflammatory conditions (12–14). Interestingly, both in vivo-generated DC-SIGN$^+$

Significance

Following exposure to inflammation, monocytes have the potential to differentiate into macrophages or monocyte-derived dendritic cells (MoDCs), each cell type then contributing in its unique way to the ensuing immune response. The molecular process guiding this differentiation is poorly defined. We show that, in monocytes, the transcription factor NR4A3 regulates a genetic program that enforces MoDC over macrophage identity and is required for the generation of MoDCs. Additionally, NR4A3-dependent MoDCs were required to mount a proper CD8$^+$ T cell adaptive immune response to gram-negative bacteria. We therefore elucidate one of the first essential transcriptional regulators of MoDC differentiation and demonstrate the biological significance of these cells.

Author contributions: S.B., J.-F.D., C.C., and N.L. designed research; S.B., J.-F.D., L.O., A.-N.P., and T.J.Y. performed research; S.B., J.-F.D., L.O., A.-N.P., and C.C. analyzed data; and S.B., S.L., and N.L. wrote the paper.

The authors declare no conflict of interest.

This article is a PNAS Direct Submission.

Data deposition: The data reported in this paper have been deposited in the Gene Expression Omnibus (GEO) database, https://www.ncbi.nlm.nih.gov/geo (GSE99837).

[1]To whom correspondence may be addressed. Email: nathalie.labrecque@umontreal.ca.

This article contains supporting information online at www.pnas.org/lookup/suppl/doi:10.1073/pnas.1821296116/-/DCSupplemental.

Published online July 8, 2019.

MoDCs and MoDCs obtained from in vitro cultures of isolated monocytes with GM-CSF and IL-4 (hereafter GM-CSF+IL-4) generate *Zbtb46*-transcribing cells (12, 15). These observations could suggest that MoDCs are part of the DC family, as opposed to activated macrophages. In addition, MoDCs are enriched for the DC but not the macrophage signature, further suggesting that they represent true DCs (16–18).

In GM-CSF+IL-4 cultures, at least two populations, recently termed GM-DC and GM-Mac, are produced (18). The GM-DC population, defined by elevated expression of MHCII and decreased CD11b surface expression, is superior in its antigen presentation capacity and is transcriptionally enriched in DC-associated genes, including *Zbtb46*. In contrast, the MHCII^{int}CD11b^{hi} GM-Mac cells bear both functional and transcriptional macrophage-like properties. Interestingly, GM-CSF+IL-4 drives the expression of nuclear orphan receptor *Nr4a3* in both human and mouse monocyte cultures (15, 19), where *Nr4a3* is most strongly expressed in the MHCII^{hi} subset (publicly available data in refs. 18 and 20). These results suggest that NR4A3 may play a role in the differentiation of MoDCs.

The NR4A nuclear orphan receptors, NR4A1-3, are transcription factors whose expression is rapidly induced following a variety of stimuli (21). Several roles have been suggested for NR4A nuclear orphan receptor family members within the myeloid lineage. Mice lacking the expression of both NR4A1 and NR4A3 rapidly develop acute myeloid leukemia (22) and NR4A1, a close homolog of NR4A3, was shown to control the generation of the Ly6C^{lo} monocyte subset and some macrophage functions (23, 24). However, the specific role of NR4A3 in monocytes has not been investigated and only recently was a role attributed for NR4A3 in DC migration (25).

Here, we have uncovered an essential role for NR4A3 in the differentiation of DC-SIGN$^+$ MoDCs following in vivo LPS injection. Moreover, we demonstrate that naive CD8$^+$ T cell priming to LPS-expressing bacteria is severely compromised in *Nr4a3*$^{-/-}$ mice, probably as a consequence of ineffective MoDC differentiation. NR4A3 was also required for the in vitro generation of MoDCs in GM-CSF+IL-4 culture and, in its absence, differentiation is diverted to a macrophage fate. Comparative transcriptomic analysis of *Nr4a3*$^{+/+}$ and *Nr4a3*$^{-/-}$ monocyte differentiation into MoDCs has allowed us to reveal an unforeseen parallel between the gene-expression program induced by NR4A3 and the migratory DC signature. We further demonstrate that *Nr4a3* transcription is downstream of IRF4.

Results

NR4A3 Is Required for the In Vitro Differentiation of GM-CSF+IL-4 MoDCs. Infection and inflammation promote the massive in vivo differentiation of monocytes into MoDCs (7–11). Furthermore, monocytes can also differentiate into MoDCs following in vitro culture with GM-CSF and IL-4 (18). This offers a unique system to better define the molecular events controlling MoDC differentiation and the role of NR4A3 in this process. Although *Nr4a3*$^{-/-}$ cells expressed normal levels of IL-4 and GM-CSF receptors (*SI Appendix*, Fig. S1 *A* and *B*), we found that NR4A3 deficiency significantly reduced (approximately 9-fold) the number of BMDCs recovered in GM-CSF+IL-4 cultures (Fig. 1*A*). This was not a consequence of reduced proliferation during the differentiation of the culture (*SI Appendix*, Fig. S1*C*). In contrast, the in vitro differentiation of CDPs into cDCs (CD8α$^+$ cDCs and CD8α$^-$ cDCs) and pDCs that occurs following culture with FLT3L (2, 26, 27) was unaffected for *Nr4a3*$^{-/-}$ BM cells (Fig. 1 *B* and *C*). Similar results were obtained using an improved FLT3L differentiation protocol where Notch signal is provided (*SI Appendix*, Fig. S1*D* and *E*) (28). This suggests that NR4A3 selectively promotes the differentiation of monocytes into DCs.

Different BM progenitors—including MDPs, common monocyte progenitors (cMoPs), CDPs, and monocytes—contribute with different efficiency to the generation of BMDCs in GM-CSF+IL-4 cultures (18). No significant differences in the frequency of these progenitors in the BM of *Nr4a3*$^{+/+}$ and *Nr4a3*$^{-/-}$ mice were found

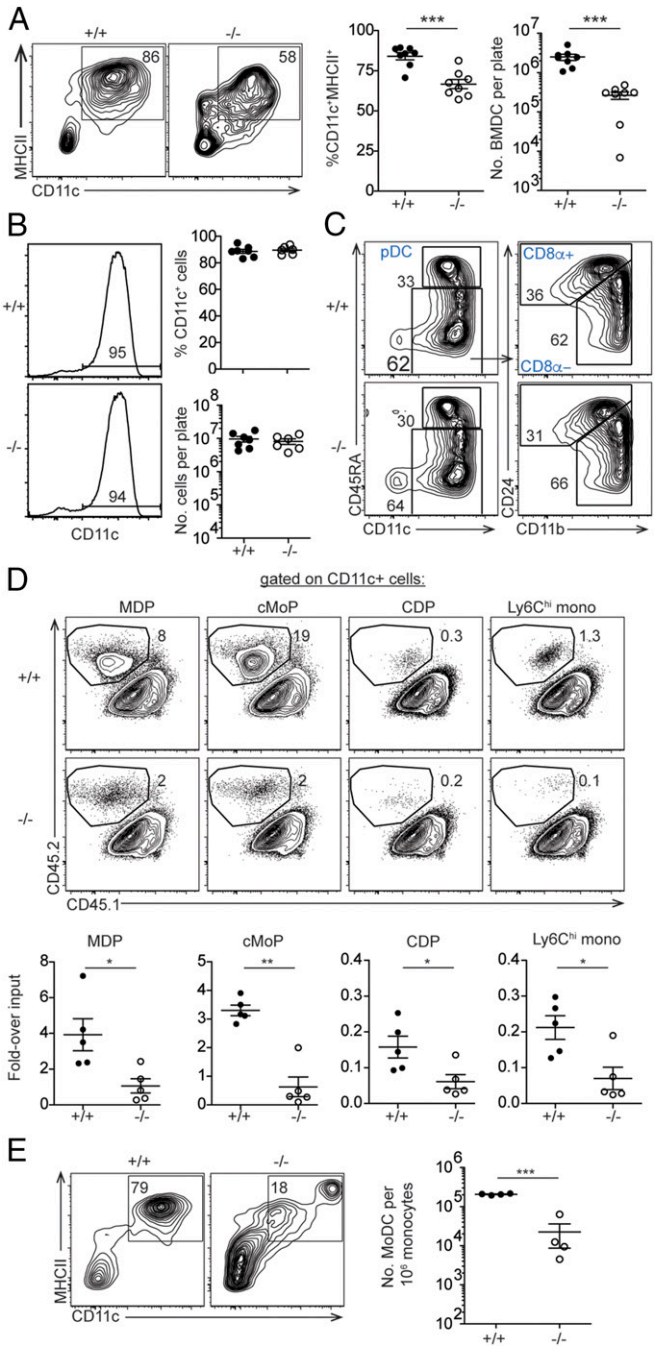

Fig. 1. NR4A3 is required for the in vitro generation of GM-CSF+IL-4 MoDCs but is dispensable for FLT3L-generated DCs. (*A* and *B*) BM cells from *Nr4a3*$^{+/+}$ and *Nr4a3*$^{-/-}$ mice were cultured for 7 d with GM-CSF+IL-4 (*A*) or 8 d with FLT3L (*B*). (*C*) Analysis of the proportion of plasmacytoid DC, CD8α$^+$, and CD8α$^-$ subpopulations of DCs obtained at the end of the culture of *Nr4a3*$^{+/+}$ and *Nr4a3*$^{-/-}$ BM cells with FLT3L. (*D*) 10^4 CD45.2$^+$ *Nr4a3*$^{+/+}$ or $^{-/-}$ MDP, cMoP, CDP, and Ly6C^{hi} monocytes were sorted and cultured for 7 d with GM-CSF and IL-4 on CD45.1$^+$ total BM cells. The proportion of CD45.2$^+$ cells within CD11c$^+$ cells (which are MHCII$^+$) (*SI Appendix*, Fig. S1*H*) is shown for each progenitor population. Shown at the bottom of the panel is the fold-increase in the cellularity of CD11c$^+$ cells over input of indicated sorted progenitors. (*E*) Sorted BM monocytes were cultured with GM-CSF+IL-4 for 7 d and analyzed by flow cytometry for the proportion and number of generated CD11c$^+$MHCII$^+$ DCs. Each symbol represents culture from an individual mouse (*A*, *B*, and *E*) or is the average of 2 or 3 replicates from a single experiment (*D*). Unpaired Student's *t* test (*A*, *B*, *D*, and *E*). Data are pooled from at least 3 independent experiments (*A*, *B*, *D*, and *E*) or 1 representative example from these experiments is shown (*C* and *D*). *$P < 0.05$, **$P < 0.01$, ***$P < 0.001$.

(*SI Appendix*, Fig. S1 *F* and *G*). We thus tested the potential of progenitors from *Nr4a3*$^{-/-}$ mice to differentiate into BMDCs by adding sorted CD45.2^{+} MDPs, cMoPs, CDPs, or monocytes (*SI Appendix*, Fig. S1*F*) to CD45.1^{+} feeder cells in GM-CSF+IL-4 cultures (18). We observed that all *Nr4a3*$^{-/-}$ progenitors had a decreased capacity to generate DCs (CD11c^{+}MHCII^{+}) after 7 d of culture (*SI Appendix*, Fig. S1*H*), and that the differences were more pronounced in progenitors with monocytic potential (MDP, cMoP, and monocytes) in comparison with CDPs and pre-DCs (Fig. 1*D* and *SI Appendix*, Fig. S1*I*). When taking into account their intrinsic capacity to expand (expressed by the "fold over input" value) and the initial frequency of the progenitors in the BM, cMoPs, and monocytes were largely responsible for the decreased number of BMDCs obtained in cultures from bulk *Nr4a3*$^{-/-}$ BM cells while CDP contribution was negligible (*SI Appendix*, Table S1). Finally, the defect of generation of BMDCs in *Nr4a3*$^{-/-}$ mice was also observed when cultures were performed using monocytes as precursors (Fig. 1*E*). Taken together, these data are consistent with the hypothesis that NR4A3 is specifically required for the differentiation of MoDCs.

NR4A3 Deficiency Diverts Differentiation to the Macrophage Lineage. Based on MHCII expression, BMDCs generated with GM-CSF+IL-4 can be classified into at least 2 populations (18). MHCII^{int} cells have a transcriptomic, phenotypic and functional profile that is more akin to macrophages (termed GM-Mac), while MHCII^{hi} cells resemble proper DCs (GM-DCs). We observed altered expression of MHCII on *Nr4a3*$^{-/-}$ BMDCs, resulting in an increase in the proportion of MHCII^{int} cells (Fig. 1*A* and *SI Appendix*, Fig. S2 *B* and *C*). This was accompanied by an increase in macrophage-associated markers F4/80, CD64, CD11b, and Mertk on *Nr4a3*$^{-/-}$ BMDCs and a decrease in the GM-DC–associated molecules (Fig. 2*A*). These results were recapitulated with cultures from sorted monocytes (*SI Appendix*, Fig. S2*A*). Although there are more GM-Mac cells in the *Nr4a3*$^{-/-}$ culture, altered expression of macrophage markers can be observed in both MHCII^{int} and MHCII^{hi} populations (*SI Appendix*, Fig. S2*B*), which have expected phenotypes (18), including for transcription factors ZBTB46, PU.1, IRF4, and IRF8, important in macrophage and DC function and differentiation. Similar results were obtained when IL-4 was omitted from the BMDC differentiation culture (*SI Appendix*, Fig. S2 *D*–*G*), suggesting that defective MoDC differentiation cannot be solely attributed to defective IL-4 signaling in *Nr4a3*$^{-/-}$ cells. Additionally, the gene signature of CD11c^{+}MHCII^{+} cells in *Nr4a3*$^{-/-}$ cultures showed enrichment in macrophage-associated transcripts *Mertk*, *Ctsl*, *Pla2g4a*, *Cd164*, *Tbxas1*, *Tcn2*, and *Dok3* (Fig. 2*B*), while the DC-associated transcripts, *Flt3*, *Traf1*, *Ccr7*, *Rab30*, and *Adam19* were decreased (Fig. 2*B*) (29, 30). This is also reflected at the morphological level with *Nr4a3*$^{-/-}$ BMDCs bearing fewer dendrites, a characteristic feature of DCs (Fig. 2*C*). Finally, when excluding CD11c^{+}MHCII^{+} cells expressing the macrophage markers CD64 and F4/80 from analysis, a more pronounced decrease (20-fold) in the generation of BMDCs is observed in the absence of NR4A3 (Fig. 2*D*). Therefore, NR4A3 appears essential specifically for the in vitro generation of CD11c^{+}MHCII^{hi} GM-DCs.

As might be expected for cells with macrophage characteristics, *Nr4a3*$^{-/-}$ cells from GM-CSF+IL-4 differentiation culture were not efficient at stimulating naive CD8^{+} OT-I T cells with the ovalbumin (OVA) (SIINFEKL) peptide (Fig. 2*E* and *SI Appendix*, Fig. S2*H*) and were less efficient at cross-presenting OVA to OT-I T cells (*SI Appendix*, Fig. S2 *I* and *J*) (18, 20). This defect in Ag presentation to naive CD8^{+} T cells is not the consequence of change in the expression level of MHCI molecules (Fig. 2*F*). Altogether, these results demonstrate a critical role for NR4A3 during monocyte-derived BMDC differentiation.

NR4A3 Is Necessary for the Differentiation of DC-SIGN^{+} MoDCs. BMDCs generated with GM-CSF+IL-4 in vitro are reminiscent of DC-SIGN^{+} MoDCs found in vivo as both express DC-SIGN, CD11b, Sirpα, and high levels of MHCII (7). In addition, both cell types are highly efficient at antigen presentation and cross-presentation (7, 15). Because NR4A3 is required for the in vitro differentiation of GM-CSF+/−IL-4 BMDCs of monocytic origin, we postulated that NR4A3 would have a role in the differentiation

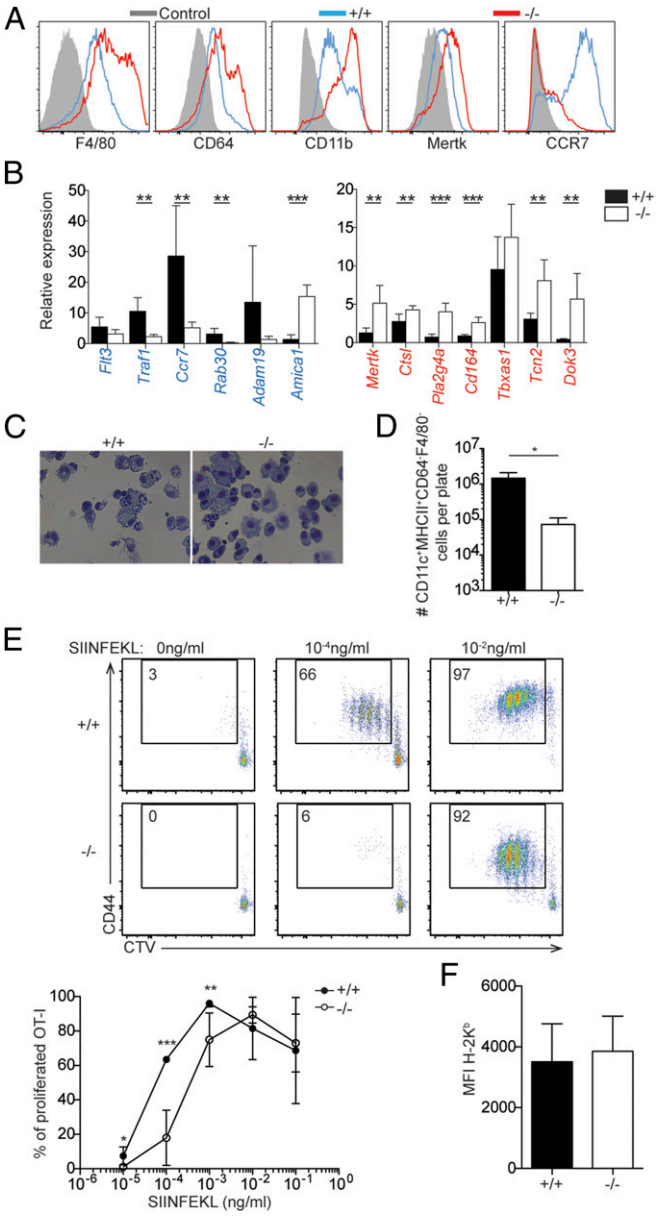

Fig. 2. *Nr4a3*-deficient cells acquire macrophage characteristics upon differentiation with GM-CSF and IL-4. (*A*) Analysis of *Nr4a3*$^{+/+}$ and $^{-/-}$ BMDCs for macrophage- (F4/80, CD64, CD11b, Mertk) and DC-associated (CCR7) molecules. Control indicates isotype or streptavidin-only controls (CCR7). (*B*) qRT-PCR on sorted CD11c^{+}MHCII^{+} cells from *Nr4a3*$^{+/+}$ and *Nr4a3*$^{-/-}$ BMDCs for genes associated with DC- (blue) and macrophage- (red) associated signature genes. (*C*) Morphology of *Nr4a3*$^{+/+}$ and $^{-/-}$ BMDCs stained with Wright–Giemsa. (*D*) Number of cells with a DC phenotype (CD11c^{+}MHCII^{+}CD64^{-}F4/80^{-}) generated in *Nr4a3*$^{+/+}$ and *Nr4a3*$^{-/-}$ cultures. (*E*) CTV-labeled OT-I T cells were cultured for 3 d with *Nr4a3*$^{+/+}$ or *Nr4a3*$^{-/-}$ BMDCs loaded with the indicated concentration of OVA peptide (SIINFEKL). Proliferation of OT-I T cells was evaluated as the percent of CD44^{hi}CTV^{lo} cells. (*F*) Expression of the MHCI molecule H-2K^{b} on *Nr4a3*$^{+/+}$ or *Nr4a3*$^{-/-}$ BMDCs generated after 7 d of culture with IL-4 and GM-CSF. Unpaired Student's *t* test (*B*, *D*, *E*, and *F*). Data are from at least 2 independent experiments with each 3 to 4 biological (*B*, *D*, and *F*) or technical (*E*) replicates or are a representative of 3 experiments (*A* and *C*). *$P < 0.05$, **$P < 0.01$, ***$P < 0.001$.

of in vivo LPS-induced DC-SIGN$^+$ DCs, which have been suggested to differentiate from monocytes (7). Indeed, adoptive transfer of monocytes followed by LPS injection leads to the generation of DC-SIGN$^+$ MoDCs (7). However, this was challenged in a study showing a reduction in the LPS-induced differentiation of DC-SIGN$^+$ DCs in *Flt3l*-deficient mice, arguing for a CDP origin for these DCs (13). A more recent study possibly reconciles these discordant findings by demonstrating that a subset of monocytes expresses FLT3 (CD135) and that this subset can differentiate in vitro into DC-SIGN$^+$ DCs with GM-CSF (10). Therefore, we used different approaches to validate the monocytic origin of DC-SIGN$^+$ DC.

First, we used unsupervised analysis of flow cytometry data to better define the cell surface phenotype of DC-SIGN$^+$ DCs. The expression of CD11c was used to identify 3 distinct subsets (R1 to R3). By comparing the subsets of cells positive for CD11c following PBS versus LPS injection, we could clearly identify that the subset R3 contains most of the LPS-induced DCs (Fig. 3*A*). The R1 and R2 subsets distinguish cDC1 (XCR1$^+$) and cDC2 subsets (Sirpα$^+$) both in PBS- and LPS-treated mice (Fig. 3*A* and *SI Appendix*, Fig. S3*A*). Importantly, DC-SIGN expression is restricted to the R3 subset (Fig. 3*A*), which expresses a profile characteristic of monocyte-derived DC, namely DC markers CD11c and CD26, monocyte/macrophage markers CD14, CD64, and F4/80, and high levels of MHCII molecules (Fig. 3*A*). We also used a directed gating strategy that distinguishes DCs of CDP versus monocyte origin based on expression of lineage-associated markers (CD64$^-$F4/80$^{+/-}$ for CDP and CD64$^+$F4/80$^+$ for monocyte origin) on mature cells as described by Guilliams et al. (31). We find that DC-SIGN$^+$ DCs are enriched within the CD64$^+$F4/80$^+$ fraction (Fig. 3*B*), suggesting a monocytic origin.

To further demonstrate that these cells are monocyte-derived, we performed adoptive transfer experiments of sorted monocytes. Because FLT3 expression distinguishes 2 different monocyte subsets, we adoptively transferred sorted total monocytes (FLT3$^+$ and FLT3$^-$) or FLT3$^-$ monocytes from C57BL/6 (CD45.2$^+$) BM (*SI Appendix*, Fig. S3*B*) (sorting strategy) into congenic B6.SJL recipients (CD45.1$^+$). The fate of the adoptively transferred monocytes was analyzed 1 d after LPS injection. As shown in Fig. 3*C*, we observed the generation of DC-SIGN$^+$ MoDCs (F4/80$^+$, CD64$^+$, CD11c$^+$, MHCII^{hi}, CD14$^+$, DC-SIGN$^+$) only when FLT3$^+$ monocytes were included within the transferred population. In one experiment, we were able to sort enough FLT3$^+$ monocytes to study their differentiation following adoptive transfer and LPS injection. As expected, these cells generated DC-SIGN$^+$ DCs (*SI Appendix*, Fig. S3*C*). The adoptive transfer of sorted pre-DCs did not generate DC-SIGN$^+$ DCs (*SI Appendix*, Fig. S3*D*). These data allow us to conclude that DC-SIGN$^+$ DCs are monocyte-derived.

The monocytic origin of DC-SIGN$^+$ DCs, lead us to evaluate whether NR4A3 was required for the differentiation of this MoDC subset. Upon intravenous LPS injection, DC-SIGN$^+$ MoDCs were virtually absent from skLNs of *Nr4a3*$^{-/-}$ mice relative to *Nr4a3*$^{+/+}$ mice (Fig. 4*A*). By using CD14, CD206, and Sirpα as alternate cell surface markers to identify DC-SIGN$^+$ MoDCs, we validated that NR4A3 affects the generation of these cells and does not solely regulate DC-SIGN expression (Fig. 4*B*). The lack of generation of DC-SIGN$^+$ MoDCs in the absence of NR4A3 was confirmed using unsupervised analysis of cytometry data (*SI Appendix*, Fig. S4*A*). Furthermore, no DC-SIGN$^+$ MoDCs were generated following the adoptive transfer of *Nr4a3*$^{-/-}$ monocytes (*SI Appendix*, Fig. S4*B*). MoDCs can also be found in the spleen (10). As expected, the number of DC-SIGN$^+$ MoDCs was also decreased in the spleen of LPS-injected *Nr4a3*$^{-/-}$ mice, suggesting that this phenotype was not specific to LNs (Fig. 4*C* and *SI Appendix*, Fig. S4*C*). Finally, the generation of DC-SIGN$^+$ MoDCs was also abrogated in the draining skLN of *Nr4a3*$^{-/-}$ mice injected locally subcutaneously with live LPS-producing *Escherichia coli* (Fig. 4*D*). Thus, *Nr4a3* plays an essential role in the generation of LPS-induced DC-SIGN$^+$ MoDCs in vivo.

Hematopoietic Requirement for NR4A3 in the Generation of DC-SIGN$^+$ MoDCs. To determine if the defective differentiation of DC-SIGN$^+$ MoDCs in the absence of NR4A3 was cell-autonomous, we transferred a 1:1 mixture of *Nr4a3*$^{+/+}$ (CD45.1$^+$) and *Nr4a3*$^{-/-}$ (CD45.2$^+$) BM cells into lethally irradiated CD45.1$^+$CD45.2$^+$ hosts. *Nr4a3*$^{-/-}$ BM was more efficient than WT BM at reconstituting most immune cell compartments, including skLN resident DCs, splenic DCs, monocytes, macrophages, neutrophils, and B cells (Fig. 4*E* and *SI Appendix*, Fig. S4*D*). However, when chimeras were injected intravenously with LPS, the DC-SIGN$^+$ MoDCs were almost exclusively of WT origin (Fig. 4*E*). Therefore, NR4A3 is required in hematopoietic cells for the generation of DC-SIGN$^+$ MoDCs and not for the generation of cDCs.

Defective Priming of Naive CD8$^+$ T Cells to *E. coli* in the Absence of NR4A3. DC-SIGN$^+$ MoDCs induced following LPS injection are efficient at priming ex vivo T cell responses and can do so by cross-presentation (7). However, their in vivo priming ability has never been demonstrated. To evaluate the in vivo consequence of the absence of DC-SIGN$^+$ MoDCs, we tested the capacity of *Nr4a3*$^{-/-}$ mice to induce the response of naive CD8$^+$ T cells upon infection with gram-negative bacteria. *Nr4a3*$^{+/+}$ 5-(and 6)-Carboxyfluorescein diacetate succinimidyl ester (CFSE)-labeled OVA-specific OT-I T cells were adoptively transferred into *Nr4a3*$^{+/+}$ and *Nr4a3*$^{-/-}$ hosts that were subsequently infected subcutaneously with an OVA-expressing strain of *E. coli*. OT-I T cells transferred into WT but not knockout (KO) recipients mounted a significant proliferative response in the draining LNs (Fig. 4*F*). To evaluate whether defective CD8$^+$ T cell priming was a consequence of the absence of DC-SIGN$^+$ MoDCs, we sorted the different DC populations present in the draining skLNs of *E. coli* OVA-infected WT mice (24 h after subcutaneous infection). Sorted DC subsets included CD11c^{hi}MHCII^{int} resident DCs, different subclasses of CD11c^{int}MHCII^{hi} migratory DCs and DC-SIGN$^+$ MoDCs. The latter were the most potent at stimulating naive CD8$^+$ T cells (Fig. 4*G*), suggesting that their absence in *Nr4a3*$^{-/-}$ mice might explain the defect in CD8$^+$ T cell priming. Importantly, *Nr4a3*$^{-/-}$ mice do not have a generalized defect in T cell priming, as they mounted a normal T cell response following infection with an OVA-expressing strain of the gram-positive bacteria *Listeria monocytogenes* (*Lm*-OVA) (*SI Appendix*, Fig. S4*E*), which does not induce the generation of DC-SIGN$^+$ MoDCs (7). Therefore, NR4A3 is required for the generation of LPS-induced DC-SIGN$^+$ MoDCs, which can stimulate an in vivo CD8$^+$ T cell response in this context. However, because we used mice with a germline deletion of *Nr4a3*, we cannot exclude that other cells could be affected and contribute to our phenotype.

Normal Differentiation of Monocytes, Macrophages, cDCs, and pDCs in *Nr4a3*$^{-/-}$ Mice. The known role of the nuclear receptor NR4A1 in monocyte differentiation (23) raises the question whether the absence of DC-SIGN$^+$ MoDCs in *Nr4a3*-deficient mice resulted from a defect in the monocyte lineage that occurred before their differentiation into DCs. However, we found similar frequencies of monocytes, both Ly6C^{hi} and Ly6C^{lo}, in the blood, BM, spleen, and LN of *Nr4a3*$^{+/+}$ and *Nr4a3*$^{-/-}$ mice (Fig. 5 *A* and *B* and *SI Appendix*, Fig. S5 *A* and *B*), and these cells expressed similar levels of CCR2, CD14, CD62L, and CCR7 (*SI Appendix*, Fig. S5*C*). Therefore, unlike its family member NR4A1, NR4A3 is not required for the differentiation of Ly6C^{lo} monocytes. There was also no difference in the frequency of CD135$^+$ monocytes in *Nr4a3*$^{+/+}$ and *Nr4a3*$^{-/-}$ mice (*SI Appendix*, Fig. S5*D*).

MoDCs have also been observed in the skin and peritoneal cavity of mice at steady state (8, 9, 32). It is unclear how similar these cells are, as they are located in different tissues, but they are likely generated by environmental cues that induce an *Ahr*-dependent differentiation process (9). We thus tested whether NR4A3 was required for the generation of these known MoDC subsets. We found no defect in the generation of skin or peritoneal MoDCs in *Nr4a3*$^{-/-}$ mice (*SI Appendix*, Fig. S5 *E*–*H*). We conclude that NR4A3 is not required for steady-state MoDCs.

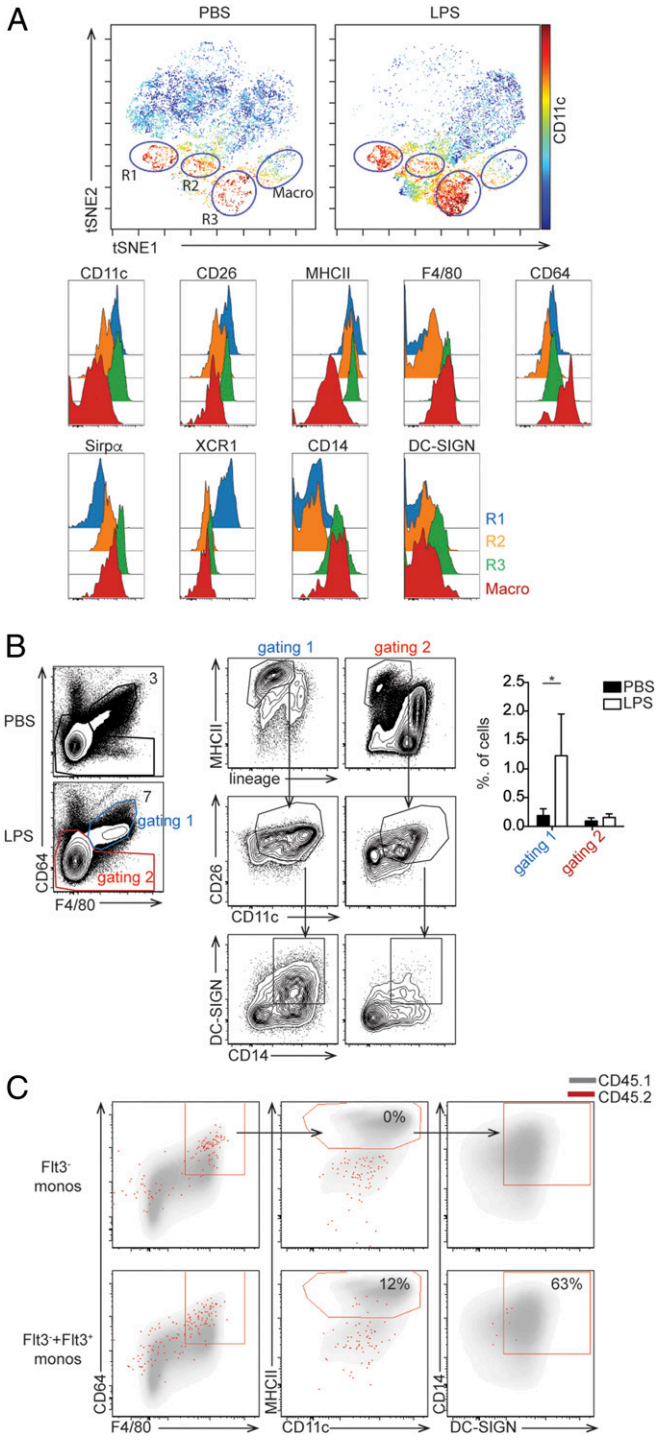

Fig. 3. Monocytic origin of LPS-induced DC-SIGN$^+$ DCs. (*A*, *Upper*) Nonlinear dimensionality reduction analysis of Lin$^-$ (CD3, CD19, B220, NK1.1) cells isolated from the skLN of mice treated with PBS or LPS. Maps are based on CD64, DC-SIGN, MHCII, CD14, SIRPα, CD11c, CD26, XCR1, and F4/80 parameters and color scale indicates CD11c expression. Elevated expression of CD11c was used to manually identify three distinct subsets (R1 to R3) while macrophage gate (Macro) was based on lack of CD11c expression with high expression of CD64, CD14, and F4/80. (*Lower*) Overlay histograms for the expression of different molecules by R1, R2, R3, and Macro populations. (*B*) Flow cytometry example and compilation for the frequency of manually gated F4/80$^+$CD64$^+$MHCII$^+$Lin$^-$CD11c$^+$CD26$^+$CD14$^+$DC-SIGN$^+$ DCs and F4/80$^-$CD64$^-$MHCII$^+$Lin$^-$CD11c$^+$CD26$^+$CD14$^+$DC-SIGN$^+$ DCs. (*C*) The 10^6 CD45.2$^+$ sorted FLT3$^-$ or FLT3$^-$+FLT3$^+$ monocytes were adoptively transferred into CD45.1$^+$ recipients a day before LPS-treatment. Twenty-four hours after LPS injection, the generation of CD45.2$^+$ (red) DC-SIGN$^+$ MoDCs (Lin$^-$CD45.2$^+$F4/80$^+$CD64$^+$MHCII$^+$CD11c$^+$CD14$^+$DC-SIGN$^+$) was evaluated by flow cytometry. CD45.2$^+$ cells are overlaid onto endogenous cells from the same gating strategy. Data shown are pooled from 2 samples. Unpaired Student's *t* test (*B*). Data are from 2 (*B*) or 3 (*C*) independent experiments with 3 biological replicates (*B*) or 1 to 3 biological replicates (*C*). *$P < 0.05$.

In specific non-LPS–driven inflammatory conditions, such as *L. monocytogenes* infection, monocytes become activated, up-regulate CD11c and MHCII molecules, and produce TNF-α and inducible nitric oxide synthase (iNOS) (14, 33). *Nr4a3*-deficient mice were infected intravenously with *L. monocytogenes* to measure the importance of NR4A3 in the production of these inflammatory monocytes, which are distinct from MoDCs, as suggested by genetic tracing experiments for *Zbtb46* and *Clec9a* (13, 14). Three days postinfection, we found no differences in the frequency of inflammatory monocytes between *Nr4a3*$^{+/+}$ and *Nr4a3*$^{-/-}$ mice (Fig. 5*C*). The fact that bacterial control was also similar in both groups suggests that *Nr4a3*$^{-/-}$ mice mounted a functional response (Fig. 5*D*). Thus, NR4A3-deficient monocytes can effectively differentiate into inflammatory monocytes. Furthermore, these results also highlight that cDC1 (CD8α$^+$) are not affected by NR4A3-deficiency as this subset is crucial for propagation of *Listeria* infection (34, 35).

Finally, given the close relationship between monocytes and macrophages, we looked at whether deficiency in NR4A3 affected macrophage generation. In the spleen, formation of red pulp (F4/80^{hi}), metallophilic (SER4$^+$), and marginal zone (22D1$^+$) macrophages appeared normal in *Nr4a3*-deficient mice (Fig. 5 *E* and *F*) and in mixed BM chimeras (*SI Appendix*, Fig. S4*D*). Thus, NR4A3 controls the differentiation of monocytes into DC-SIGN$^+$ DCs without contributing to the differentiation of Ly6C^{lo} monocytes, steady-state MoDCs, inflammatory monocytes, and macrophages.

We then evaluated whether NR4A3 was involved in the differentiation of pDCs and cDCs. We found no difference in the percentage and number of pDCs within the spleen, BM, and LNs of *Nr4a3*$^{+/+}$ and *Nr4a3*$^{-/-}$ mice (Fig. 5*G*). Similarly, the cDC1 (XCR1$^+$) and cDC2 (Sirpα$^+$) subsets were not affected by NR4A3 deficiency in the spleen and BM (Fig. 5*H* and *SI Appendix*, Fig. S6*A*). There was, however, a difference in the number of cDC in the LNs of *Nr4a3*$^{-/-}$ mice, which was a direct consequence of the reduced pool of migratory DCs that is observed in the LNs of *Nr4a3*$^{-/-}$ (Fig. 5 *I* and *J* and *SI Appendix*, Fig. S6*B*), as reported by Park et al. (25); note that the staining strategy used to identify the cDC1 and cDC2 subsets in Fig. 5*H* includes both resident and migratory DCs (*SI Appendix*, Fig. S6*A*). The effect of NR4A3 on cDC migration is at least in part explained by the reduced expression of CCR7 on these cells (*SI Appendix*, Fig. S6 *C* and *D*), as previously reported (25). The normal distribution of cDCs in the skin of *Nr4a3*$^{-/-}$ mice (Fig. 5*K* and *SI Appendix*, Fig. S6*E*), as well as in other peripheral tissues (25), further supports normal development of cDCs in the absence of NR4A3. In inflammatory conditions, *Nr4a3*$^{-/-}$ splenic cDCs respond normally to LPS and *Listeria* by up-regulating the expression of CD86 and MHCII molecules (*SI Appendix*, Fig. S6 *F* and *G*). These data further support the idea that, while NR4A3 has an impact on the migration of cDCs, it is not required for their development. The importance of NR4A3 in DC differentiation seems to be restricted to the DC-SIGN$^+$ MoDC compartment.

NR4A3 Controls a Gene-Expression Profile that Distinguishes DCs and Macrophages. To further understand how NR4A3 controls the differentiation of monocytes into MoDCs, we determined the time point at which defective MoDC differentiation appears in the GM-CSF+IL-4 differentiation culture of sorted monocytes. No phenotypic differences between *Nr4a3*$^{+/+}$ and *Nr4a3*$^{-/-}$ cultures were present at day 1, while differences in expression of MHCII and CCR7 occurred at day 2 of monocyte differentiation (*SI Appendix*, Fig. S7*A*). This coincides with the induction of *Nr4a3* transcription (*SI Appendix*, Fig. S7*B*). Furthermore, no

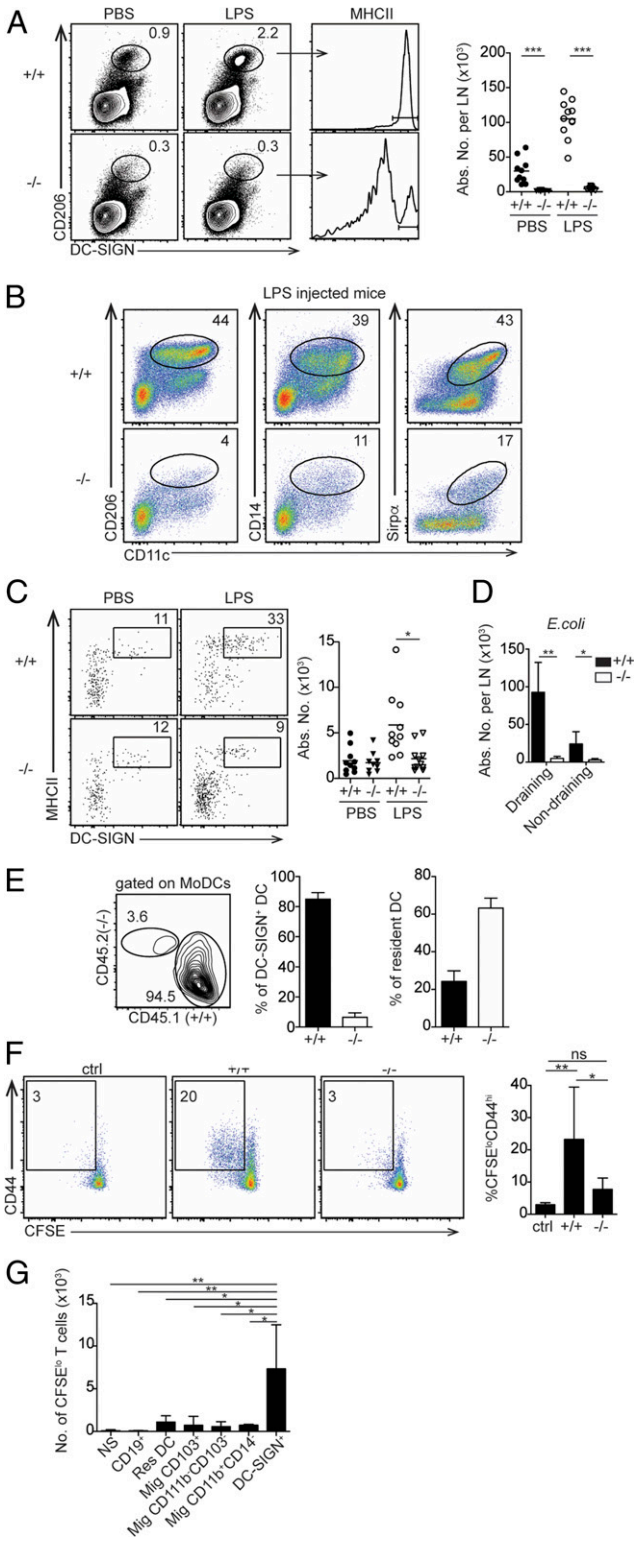

Fig. 4. NR4A3 controls in vivo DC-SIGN$^+$ MoDC differentiation. (*A*) *Nr4a3*$^{+/+}$ and *Nr4a3*$^{-/-}$ mice were injected intravenously with PBS or LPS to generate MoDCs (DC-SIGN$^+$CD206$^+$MHCII^{hi} cells) in skLNs. (*B*) Alternate strategy to identify MoDCs generated in the skLNs of LPS-injected mice. Lin$^-$ (CD3, CD19, NK1.1) cells were analyzed for the expression of CD206, CD14, or Sirpα. (*C*) Generation of DC-SIGN$^+$ DCs in the spleen of *Nr4a3*$^{+/+}$ and *Nr4a3*$^{-/-}$ mice following LPS injection. (*D*) Mice were injected subcutaneously with *E. coli* in the right flank. MoDCs were enumerated in the draining and contralateral LNs. (*E*) 1:1 *Nr4a3*$^{+/+}$ and *Nr4a3*$^{-/-}$ BM chimeras cells were injected with PBS or LPS. The relative contribution of $^{+/+}$ and $^{-/-}$ cells to MoDCs or LN resident DCs (CD11c^{hi}MHCII$^+$) was evaluated 24 h postinjection. (*F*) CFSE-labeled OT-I T cells were adoptively transferred into *Nr4a3*$^{+/+}$ and *Nr4a3*$^{-/-}$ recipients before subcutaneous injection of PBS (ctrl, WT mice) or OVA-expressing *E. coli*. OT-I proliferation in the draining LN was measured 3 d postinfection. (*G*) Twenty-four hours postinfection of WT mice with OVA-expressing *E. coli*, the indicated populations were sorted from the draining LN and incubated with CFSE-labeled OT-I cells to assess their capacity to stimulate naive CD8$^+$ T cells. Each symbol represents an individual mouse. Unpaired Student's *t* test (*A*, *C*, and *D*) or 1-way ANOVA with Tukey's post-test analysis (*F* and *G*). Data are pooled from 2 (*D* and *E*), 3 (*A*, *F*, and *G*), or 4 (*C*) independent experiments or are representative of 3 experiments (*B*). (*E*) Two mice per group per experiment; (*D* and *F*) 2 (ctrl) or 3 mice per group per experiment. *$P < 0.05$, **$P < 0.01$, ***$P < 0.001$.

difference in survival/apoptosis and proliferation was observed up to day 3 of the differentiation culture (*SI Appendix*, Fig. S1*C*). Therefore, we decided to compare the gene-expression profile, using RNA sequencing (RNA-seq), of ex vivo-sorted BM monocytes (day 0) and cells from day 1 and 2 of GM-CSF+IL-4 differentiation cultures. As shown in Fig. 6*A*, very few genes were differentially expressed between *Nr4a3*$^{+/+}$ and *Nr4a3*$^{-/-}$ monocytes and at day 1 of the differentiation culture (2 and 1, respectively). This is not surprising, as *Nr4a3* expression levels are low at these time points (*SI Appendix*, Fig. S7*B*). However, at day 2 of the differentiation culture, 216 genes were differentially expressed, 15 were up-regulated in *Nr4a3*$^{-/-}$ cells, while 201 were down-regulated (Fig. 6*A* and Dataset S1). Of these differentially expressed genes, 14 encode for transcription factors (Fig. 6*B*). Of note, most of the transcription factors known to be involved in DC differentiation (IRF4, BAFT3, E2-2, ID2, and so forth) are not differentially expressed. This suggests that NR4A3 induces a unique transcriptional network essential for the differentiation of MoDCs.

Importantly, NR4A3 deficiency did not impact the expression of IL-4 and GM-CSF receptors and their signaling components (Dataset S2). Accordingly, we did not observe any difference in expression level of the IL-4 and GM-CSF receptors by flow cytometry (*SI Appendix*, Fig. S1 *A* and *B*). Furthermore, gene set enrichment analysis did not show enrichment for the IL-4 and GM-CSF signature (PID_GMCSF_PATHWAY, false-discovery rate [FDR] = 0.7; PID_IL4_2PATHWAY, FDR = 0.95).

To confirm the role of NR4A3 in skewing the differentiation of monocytes toward a DC as opposed to a macrophage fate (as shown in Fig. 2), we performed hierarchical clustering analysis of the different DC, macrophage, and monocyte populations characterized by the Immunological Genome Project Consortium (http://www.immgen.org) (36, 37) using the differentially expressed genes (referred as the NR4A3 gene signature) identified from our RNA-seq analysis of day 2 GM-CSF+IL-4 differentiation culture of *Nr4a3*$^{-/-}$ and *Nr4a3*$^{+/+}$ monocytes. Genes within the NR4A3 gene signature were sufficient to separate the ImmGen data into 2 distinct clusters, as shown by the dendrogram atop Fig. 6*C*: 1 defined mostly by monocyte/macrophage gene-expression profiles and 1 with a large majority of DC subsets. Similarly, by displaying the fold over the mean expression data (of all of the monocyte/macrophage and DC subsets) for the top 10 up-regulated and down-regulated genes of the NR4A3 gene signature, we could show their differential expression in DCs versus monocyte/macrophage (*SI Appendix*, Fig. S7*C*). Therefore, genes regulated by NR4A3 may actively participate in promoting monocyte differentiation into MoDCs.

Our clustering analysis also reveals that expression of several genes down-regulated in *Nr4a3*$^{-/-}$ monocytes upon culture with GM-CSF+IL-4 were highly expressed in migratory DC subsets (Fig. 6*C*; see MHCII^{hi} DC populations highlighted in red). We thus sought to determine if NR4A3 regulated the DC migratory signature. To do this, we plotted the data from our RNA sequencing for 2 selected sets of genes defined by Miller et al. (30): the core migratory DC signature (Fig. 6*D*, plotted in red) and the transcriptional signature associated with tissue-resident DCs

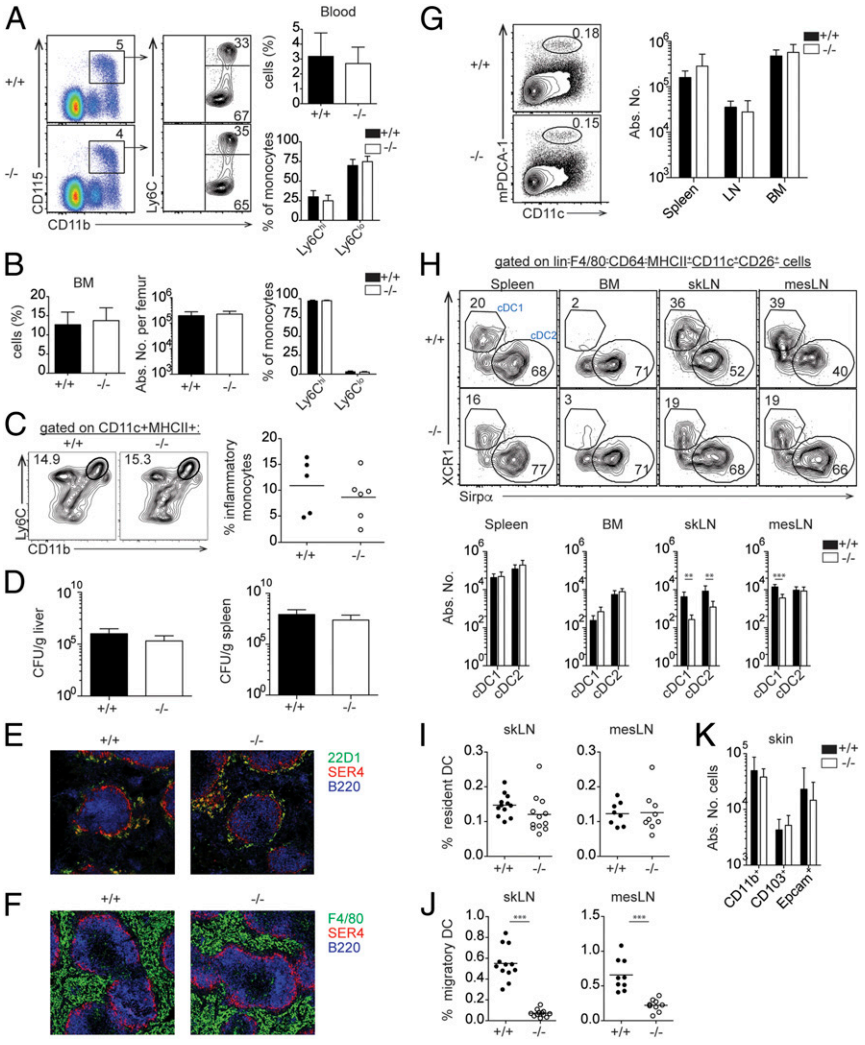

Fig. 5. Normal development of monocytes, macrophages, pDCs, and cDCs in *Nr4a3*$^{-/-}$ mice. Ly6C^{hi} and Ly6C^{lo} monocytes from the blood (*A*) and BM (*B*) were quantified by flow cytometry in *Nr4a3*$^{+/+}$ and *Nr4a3*$^{-/-}$ mice. (*C*) *Nr4a3*$^{+/+}$ and *Nr4a3*$^{-/-}$ mice were infected intravenously with *L. monocytogenes* and the generation of inflammatory monocytes in the spleen was measured 3 d later. (*D*) CFU of *L. monocytogenes* in the liver and spleen of mice infected in *C*. (*E* and *F*) Spleen sections from *Nr4a3*$^{+/+}$ and *Nr4a3*$^{-/-}$ mice were stained for B220 (blue) to reveal B cell zones and macrophage markers to visualize marginal zone (22D1), metallophilic (SER4), and red pulp (F4/80) macrophages; 100× magnification. (*G*) pDCs (CD11c^{+}mPDCA-1^{+}) were enumerated in lymphoid organs of *Nr4a3*$^{+/+}$ and *Nr4a3*$^{-/-}$ mice. (*H*) cDCs were defined as Lin^{-}(CD3, CD19, B220, NK1.1) F4/80^{-}CD64^{-}MHCII^{+}CD11c^{+}CD26^{+} cells across different lymphoid tissues. The proportion (*Upper*) and numbers (*Lower*) of cDC1 (XCR1^{+}) and cDC2 (Sirpα^{+}) subpopulations in these organs are shown. cDCs from skin-draining and mesenteric LNs (mesLN) were divided into resident (CD11c^{+}MHCII^{int}, *I*) and migratory (CD11c^{+}MHCII^{hi}, *J*) populations in *Nr4a3*$^{+/+}$ and *Nr4a3*$^{-/-}$ mice. Shown is the percent contribution of these cDCs to the total cell population in these LNs. (*K*) Number of CD11b^{+}, CD103^{+}, and Epcam^{+} DCs in the skin of *Nr4a3* sufficient and deficient mice. Each symbol represents an individual mouse. Data are pooled from 2 (*A*, *B*, *C*, *D*, and *G*) or 3 (*H*, *I*, *J*, and *K*) independent experiments with a total of 5 (*Nr4a3*$^{+/+}$ *C* and *D*) or more mice per group. $^{**}P < 0.01$, $^{***}P < 0.001$.

(Fig. 6*D*, plotted in blue: genes whose expression is up-regulated in resident DCs and strongly down-regulated in migratory DCs). Among the genes that are significantly down-regulated in *Nr4a3*$^{-/-}$ cells compared with WT cells, a high proportion (66 of 216) (plotted outside the gray area on Fig. 6*D*) are genes within the core migratory DC gene-expression signature as revealed by the fold-change of expression of these genes and their *P* value (Fig. 6*D* and Dataset S1). However, the tissue-resident DC signature (Fig. 6*D*, blue dots) was not affected by the absence of NR4A3. This is in agreement with our observation that NR4A3 deficiency does not affect the proportion and number of lymphoid organ resident DCs (Fig. 5 *H* and *I*) but does affect migratory DCs.

The IRF4-NR4A3 Axis Controls MoDC Differentiation. A recent study demonstrated that in vitro MoDC differentiation of *Irf4*-deficient monocytes led to the generation of cells with a macrophage phenotype that were unable to prime and cross-prime naive CD8^{+} T cells (15). In addition, IRF4 is known to modulate a substantial proportion of the DC migratory signature (20). We thus hypothesized that IRF4 and NR4A3 somehow interact to regulate a common transcriptional program. IRF4 protein expression was similarly induced in *Nr4a3*$^{+/+}$ and *Nr4a3*$^{-/-}$ BM differentiation culture, and data from our RNA-seq experiment showed that *Irf4* transcription was similar from day 0 to day 2 of MoDC differentiation (*SI Appendix*, Fig. S8 *A* and *B*), suggesting that NR4A3 is not required for proper IRF4 expression. However, given that one of the genes whose transcription is most down-regulated in *Irf4*$^{-/-}$ MoDC cultures is *Nr4a3* (15), an IRF4-NR4A3 axis may be important for MoDC generation in GM-CSF+IL-4 cultures. To address this, we compared the gene-expression profile induced by IRF4 and NR4A3 using the publicly available data for IRF4 (GSE75015) (15, 38) and our RNA-seq data (day 2 of differentiation). Of the genes, 216 are regulated by NR4A3 while 1,165 are regulated by IRF4 and, among the NR4A3 regulated genes, 75 are shared with the *Irf4* gene signature (35%) (Fig. 7*A*). This is likely an underestimation, as the IRF4-dataset was obtained at day 4 of culture. This suggests that part of the transcriptional program induced by IRF4 could be the consequence of *Nr4a3* transcriptional induction. Previously published IRF4 ChIP-seq data demonstrate that, in DCs, IRF4 directly targets key genes for MHCII antigen presentation, including *Ciita*, *Ctss*, and *H2-Dmb2* (20, 39). These data also suggest that IRF4 can bind 11 kb upstream of the *Nr4a3* gene in BMDCs, Th2, and Th17 cells (20, 39). To investigate whether IRF4 was directly regulating *Nr4a3* transcription, we used ChIP of IRF4 in GM-CSF+IL-4 cell cultures. Our data show that IRF4 indeed binds upstream of the *Nr4a3* gene (Fig. 7*B*).

To test whether the induction of *Nr4a3* transcription by IRF4 was a key event mediated by IRF4 to induce MoDC differentiation, we transduced *Nr4a3* into *Irf4*$^{-/-}$ BM cells. Reintroduction of NR4A3 expression in *Irf4*$^{-/-}$ cells restored their capacity to generate CD11c^{+} cells upon culture with GM-CSF and IL-4 (Fig. 7 *C* and *D*). In addition, the GM-DC markers MHCII and CCR7 were increased by NR4A3 while the expression of the GM-Mac marker, CD11b, was down-regulated (Fig. 7

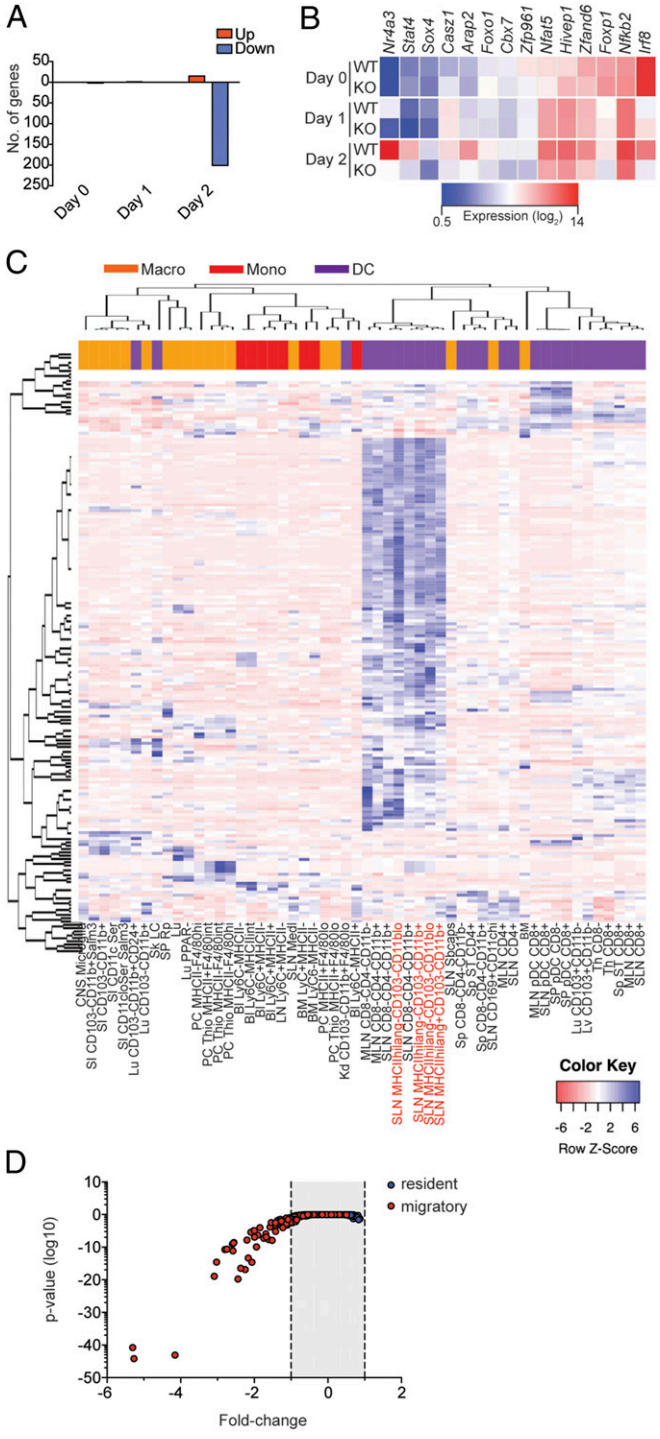

Fig. 6. NR4A3 induces an early transcriptional program required for the differentiation of MoDCs. (*A*) Monocytes were sorted and cultured for 0, 1, or 2 d with GM-CSF+IL-4 before transcriptomic analysis by RNA sequencing. The number of differentially regulated genes in *Nr4a3*$^{-/-}$ compared with WT cells is shown. (*B*) Heatmap of the transcription factors regulated by NR4A3 over the course of monocyte cultures differentiated with GM-CSF and IL-4. (*C*) Population clustering and heat map of relative transcript value for monocyte (red), macrophage (orange), and DC populations (purple) from the Immgen database based on our NR4A3 gene signature (significantly differentially expressed genes [>2-fold] from day 2 differentiated *Nr4a3*$^{+/+}$ and $^{-/-}$ monocytes). Highlighted in red are MHCII^{hi} migratory DC populations. (*D*) Gene-expression analysis of day 2 *Nr4a3*$^{+/+}$ and *Nr4a3*$^{-/-}$ GM-CSF+IL-4 MoDCs. Each dot represents the results of the differential expression analysis for 1 gene in the migratory (red) or resident (blue) DC signature as described by Miller et al. (30).

C and *D*). Finally, the transduction of *Nr4a3* increases the transcription of *Ccr7*, *Kmo*, *Traf1*, and *Fscn1* (Fig. 7*E*), all of which are part of the transcriptome regulated by IRF4 in GM-CSF+IL-4 cultures (15). In addition, *Ccr7*, *Kmo*, and *Traf1* are part of the core cDC signature and *Ccr7*, *Traf1*, and *Fscn1* are part of the migratory DC signature (30). We conclude that proper differentiation of MoDCs requires an IRF4-NR4A3–mediated transcriptional program, without which cells acquire macrophage characteristics. Moreover, these data demonstrate that NR4A3 can drive a portion of this differentiation program in the absence of IRF4.

Interestingly, DC-SIGN^{+} MoDCs are also not generated in *Irf4*$^{-/-}$ BM chimeras following in vivo LPS injection (*SI Appendix*, Fig. S8*C*), suggesting that as with in vitro GM-CSF+IL-4 differentiation culture, the IRF4-NR4A3 axis is controlling the differentiation of monocytes into DC-SIGN^{+} MoDCs.

Discussion

Our results identify NR4A3 as a transcription factor that controls the differentiation of monocytes into DCs. In the absence of NR4A3, DC-SIGN^{+} MoDCs were not generated following LPS injection. As a consequence, naive CD8^{+} T cell priming was abrogated, suggesting an essential role of this DC subset for the in vivo T cell response to gram-negative bacteria. NR4A3 was also essential for in vitro-generated GM-CSF+IL-4 BMDCs and acts as an important effector of the IRF4-driven MoDC differentiation program.

The origin of LPS-induced DC-SIGN^{+} MoDCs has remained controversial. In the initial study, their monocytic origin had been demonstrated by adoptive transfer of monocytes and by their abrogation in a LysMCre depletion experiment (7). However, subsequent studies showed that DCs induced by LPS injection expressed ZBTB46 and were affected in FLT3L-deficient mice, which suggested a CDP origin (13, 40). The fact that ZBTB46 can be expressed by MoDCs (12) and that a subset of monocytes expressing CD135 (FLT3) has been recently discovered (10), opens the possibility that all of these findings may not necessarily contradict each other. Indeed, the importance of FLT3L on the transition of CD135^{+} monocytes to MoDCs in vivo has not been thoroughly explored. In addition, while the architecture of the LN in *Flt3l*$^{-/-}$ mice is unaffected, its size and cellular composition are dramatically altered. In addition, *Flt3l*$^{-/-}$ mice have deficient hematopoiesis (41). These factors could contribute to a suboptimal response of *Flt3l*$^{-/-}$ mice to an LPS challenge.

Here, we demonstrated that LPS-induced DC-SIGN^{+} DCs express molecules associated with monocyte/macrophage lineages, such as CD64, F4/80, and CD14, as well as DC-associated molecules CD26 and CD11c, and thus segregate away from cDC1, cDC2, and macrophages in unsupervised analysis. In addition, our adoptive transfer experiments show that CD135^{+} monocytes generate such cells. Therefore, we conclude that LPS-induced DC-SIGN^{+} DCs are monocyte-derived.

Fate determination of monocytes upon activation may be guided by local inflammatory cues or may result from the existence of prespecified progenitor subsets. In favor of the second hypothesis, 2 recent studies have shown that, within monocytes, subsets exist that are more likely to generate MoDCs (10, 15). Ly6C^{hi}TREML4^{-} monocytes can give rise to ZBTB46^{+} MoDCs in GM-CSF+IL-4 cultures (15). In addition, activation of FLT3^{+} PU.1^{hi} monocytes leads to their differentiation into DC-SIGN^{+} DCs while FLT3^{-}PU.1^{lo} monocytes preferentially generate iNOS^{+} phagocytes (10). However, the fact that we found no differences in (*i*) TREML4^{-} or TREML4^{+} monocyte populations (*SI Appendix*, Fig. S5*I*); (*ii*) FLT3^{+} or FLT3^{-} monocytes; or (*iii*) in the transcriptome, including transcription of *Treml4*, *Sfpi1* (gene coding PU.1), and *Flt3* between *Nr4a3*$^{+/+}$ and *Nr4a3*$^{-/-}$ monocytes, suggests that differences in monocyte progenitors were not responsible for the decreased generation of in vivo DC-SIGN^{+} MoDCs and in vitro MoDCs in the absence of NR4A3. We conclude that

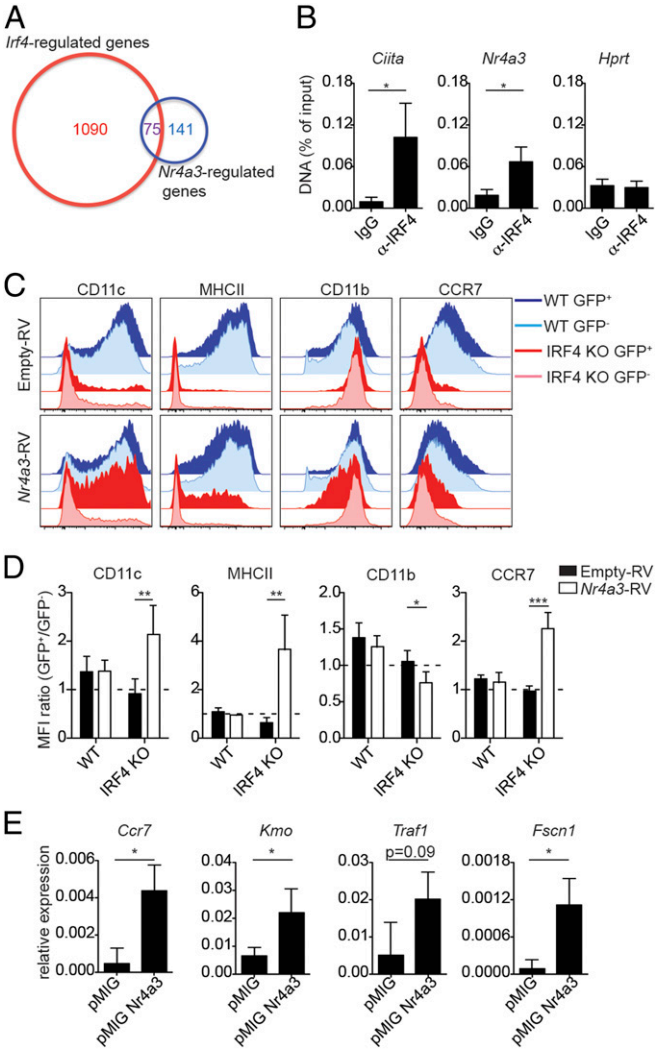

Fig. 7. Induction of *Nr4a3* transcription by IRF4 is essential for MoDC differentiation. (*A*) Venn diagram showing the overlap of genes differentially expressed in MoDC cultures between *Irf4*-deficient (GSE75015) and *Nr4a3*-deficient cells. *Irf4*-deficient cultures were analyzed on day 4, while *Nr4a3*$^{-/-}$ cultures were analyzed on day 2. (*B*) ChIP with IRF4 antibody or its isotype control on in vitro differentiated GM-CSF+IL-4 cultures followed by qPCR amplification of regions located upstream of *Ciita* (positive control), *Nr4a3*, and *Hprt* (negative control) genes. (*C*) *Irf4*-sufficient or -deficient BM cells were transduced with empty or *Nr4a3*-encoding retrovirus and then cultured for 7 d with GM-CSF+IL-4. Expression of CD11c, MHCII, CD11b, and CCR7 was then measured by flow-cytometry on transduced (GFP$^+$) and untransduced (GFP$^-$) cells. (*D*) Expression of CD11c, MHCII, CD11b and CCR7 on the transduced cells (GFP$^+$) in *C* relative to that of the untransduced (GFP$^-$) population. (*E*) mRNA relative expression of *Ccr7*, *Kmo*, *Traf1*, and *Fscn1* in *Irf4*$^{-/-}$ BM transduced with pMIG or pMIG-*Nr4a3* and then cultured with IL-4 and GM-CSF for 7 d. Unpaired Student's *t* test (*B*, *D*, and *E*). Data from *B* are from 3 independent experiments. Representative example in *C* and data pooled in *D* are from 2 independent experiments with 2 or 3 biological replicates per experiment. Data in *E* is from 3 biological replicates. $*P < 0.05$, $**P < 0.01$, $***P < 0.001$.

NR4A3 has no obvious role in the homeostasis of monocytes, in contrast to its homolog NR4A1 (23).

The nuclear receptors NR4A1 and NR4A3 share high-sequence similarity, can transactivate through the same DNA element, and can even act as heterodimers, which suggest they may have redundant functions (21). However, our data show that these molecules have very distinct roles in monocytes. The conversion of Ly6C^{hi} into Ly6C^{lo} monocytes requires the C/EBPβ-mediated induction of NR4A1, which is important for the survival of Ly6C^{lo} patrolling monocytes, as opposed to NR4A3 (23, 42). In addition, NR4A1 is dispensable for the generation of MoDCs, and the subset of monocytes expressing NR4A1 is unable to differentiate into MoDCs (15). The different roles of NR4A1 and NR4A3 in monocytes is linked to their differential expression, as only *Nr4a1* transcription is detectable in monocytes based on our RNA-seq data and the report of Briseño et al. (15). In contrast, the transcription of *Nr4a3* is induced during the differentiation of monocytes into MoDCs, while *Nr4a1* transcription is abrogated. Thus, the NR4A1 and NR4A3 homologs have nonredundant functions and seem to act in a mutually exclusive manner during MoDC differentiation.

It is becoming clearer that different MoDCs described in the literature do not necessarily function similarly. For example, skin-derived MoDCs have been shown to be somewhat inefficient at cross-presenting antigen to T cells, while LPS DC-SIGN$^+$ MoDCs, at least in vitro, are as efficient as cDCs at performing this task (7, 8). It was therefore important to clarify the role of DC-SIGN$^+$ MoDCs in vivo and our results suggest that, following infection with gram-negative bacteria, DC-SIGN$^+$ MoDCs are involved in priming a T cell response. The role of NR4A3 for the priming of a T cell response is context-dependent, as it was not required following *L. monocytogenes* infection. This may be explained by the lack of generation of DC-SIGN$^+$ MoDCs during *L. monocytogenes* infection (7). Although our results suggest an important role for DC-SIGN$^+$ MoDCs, the use of a germline deletion makes it possible that defects in other populations might contribute to our phenotype.

IRF4 is required for the in vitro differentiation of monocytes into MoDCs with efficient antigen presentation capacity (15). In the absence of IRF4, monocytes differentiate into macrophages, which are far less efficient at activating T cells. In addition, in the absence of NR4A3, the remaining cells in the BMDC culture have a macrophage morphology, phenotype and gene-expression signature, which paralleled results obtained in *Irf4*$^{-/-}$ BMDC culture. Similarities between NR4A3 and IRF4 BMDC cultures suggest an axis of regulation mediated by these proteins. The comparison of our RNA-seq data with that obtained with *Irf4*$^{-/-}$ BMDCs revealed similarities in the gene-expression program induced by IRF4 and NR4A3. Our demonstration that enforced NR4A3 expression in *Irf4*$^{-/-}$ BMDC culture was sufficient to partially restore the differentiation of MoDCs suggests that some of the IRF4-mediated effect is mediated via the direct induction of *Nr4a3* transcription. Furthermore, regulation of the expression of several transcription factors by NR4A3 suggests that IRF4-mediated induction of *Nr4a3* transcription may result in significant changes in the gene-expression program, allowing for MoDC differentiation. IRF4 is also important for the differentiation of the cDC2 subset (CD11b$^+$/Sirpα$^+$) (43). However, in this context IRF4 does not act via the induction of the transcription of *Nr4a3*, as *Nr4a3*$^{-/-}$ mice do not have any deficiency in cDC2 generation. Therefore, the induction of *Nr4a3* expression is a selective event induced by IRF4 and is required for the differentiation of MoDCs.

One of the unifying themes behind the roles for NR4A3 in DC biology seems to relate to the acquisition of the migratory DC gene-expression signature: (*i*) transcriptomic analyses have revealed that in vitro differentiated GM-DCs cluster with migratory DCs (18), (*ii*) DC-SIGN$^+$ MoDC up-regulate several genes from the migratory signature (17), and (*iii*) our RNA-seq analysis reveals that NR4A3 controls the induction of a large proportion of genes from this signature. It is interesting that both *Irf4*$^{-/-}$ and *Nr4a3*$^{-/-}$ mice have a deficiency in migratory DCs (25, 44) and it would be relevant to study whether cDC2 migration is also mediated by an IRF4-NR4A3 axis. The proper differentiation of monocytes into DCs, away from macrophages, has been previously linked to their capacity to migrate to draining LN and stimulate a T cell response (45), but it is unclear why this migratory program would be required for the production of LPS-induced MoDCs. Nonetheless, *Nr4a3*-dependent migratory differentiation of monocytes is not solely

meant to facilitate the displacement of these cells toward the LN, since *Nr4a3*$^{-/-}$ BM cells cultured with GM-CSF and IL-4 also fail to properly present antigen.

The fact that LPS-induced MoDCs seem to be uniquely coupled to an NR4A3-dependent migratory signature may also explain why we found no defect in types of MoDCs usually found at steady state, such as those from the skin or the peritoneal cavity (8, 9). Indeed, transcriptional analysis of these different MoDCs shows that genes from the DC migratory signature, such as *Ccr7*, *Fscn1*, *Traf1*, or *Socs2* are not particularly enriched in the MoDC populations that are stable in *Nr4a3*-deficient mice while they are expressed by LPS-induced DC-SIGN^{+} MoDCs (8, 16, 17, 32, 36). On the other hand, it is also possible that NR4A3 is selectively required for the differentiation of monocytes into MoDCs specifically in the context of microbial stimulation.

In this study, we uncover a unique role for the nuclear orphan receptor NR4A3 in the differentiation of monocytes into DCs both in vivo and in vitro. Moreover, NR4A3 is the one of the few transcription factors identified to date, which contributes to the differentiation of monocytes into LPS-induced DCs. Therefore, targeting the NR4A3 pathway might provide unique opportunities to improve DC vaccination strategies.

Materials and Methods

Standard procedures for cell cultures, flow cytometry, cell sorting, adoptive transfers, BM chimera generation, LPS/bacterial injections, *Nr4a3*-overexpression, and microscopy are described in *SI Appendix, Materials and Methods*. Antibodies used for flow cytometry are listed in *SI Appendix*, Table S2. qPCR was performed on cDNA from sorted CD11c^{+}MHCII^{+} cells generated in GM-CSF/IL-4 cultures and primers are listed in *SI Appendix*, Table S3. Detailed description of RNA sequencing and hierarchical clustering are also available in *SI Appendix, Materials and Methods*. The accession number for the sequencing data for RNA-seq reported in this paper is GSE99837 (46). ChIP assays were performed according to the manufacturer's instructions (Transcription factor kit, Diagenode) and primers are described in *SI Appendix, Material and Methods*. All mice were housed in a pathogen-free environment and treated in accordance to the Canadian Council on Animal Care guidelines. In all experiments, data are presented as mean ± SD if not stated otherwise.

Additional information is provided in *SI Appendix, Materials and Methods*.

ACKNOWLEDGMENTS. We thank members of the laboratory for helpful discussion; Martine Dupuis for cell sorting; the animal care facility for mice husbandry; Dr. Orla M. Conneely for *Nr4a3*$^{-/-}$ mice, and Dr. Tak W. Mak for *Irf4*$^{-/-}$ mice; Jennifer Huber, Florent Guilloteau, and Patrick Gendron for RNA sequencing experiments and analysis; and Drs. Heather Melichar, Christopher Rudd, Nicolas Cermakian, and Connie M. Krawczyk for critical reading of the manuscript. This work was funded by the Canadian Institutes of Health Research (MOP-142333).

1. B. Cisse *et al.*, Transcription factor E2-2 is an essential and specific regulator of plasmacytoid dendritic cell development. *Cell* **135**, 37–48 (2008).
2. S. H. Naik *et al.*, Development of plasmacytoid and conventional dendritic cell subtypes from single precursor cells derived in vitro and in vivo. *Nat. Immunol.* **8**, 1217–1226 (2007).
3. T. L. Murphy *et al.*, Transcriptional control of dendritic cell development. *Annu. Rev. Immunol.* **34**, 93–119 (2016).
4. S. Iborra *et al.*, Optimal generation of tissue-resident but not circulating memory T cells during viral infection requires crosspriming by DNGR-1^{+} dendritic cells. *Immunity* **45**, 847–860 (2016).
5. K. Hildner *et al.*, Batf3 deficiency reveals a critical role for CD8alpha+ dendritic cells in cytotoxic T cell immunity. *Science* **322**, 1097–1100 (2008).
6. A. T. Satpathy *et al.*, Notch2-dependent classical dendritic cells orchestrate intestinal immunity to attaching-and-effacing bacterial pathogens. *Nat. Immunol.* **14**, 937–948 (2013).
7. C. Cheong *et al.*, Microbial stimulation fully differentiates monocytes to DC-SIGN/CD209(+) dendritic cells for immune T cell areas. *Cell* **143**, 416–429 (2010).
8. S. Tamoutounour *et al.*, Origins and functional specialization of macrophages and of conventional and monocyte-derived dendritic cells in mouse skin. *Immunity* **39**, 925–938 (2013).
9. C. Goudot *et al.*, Aryl hydrocarbon receptor controls monocyte differentiation into dendritic cells versus macrophages. *Immunity* **47**, 582–596.e6 (2017).
10. S. Menezes *et al.*, The heterogeneity of Ly6C^{hi} monocytes controls their differentiation into iNOS^{+} macrophages or monocyte-derived dendritic cells. *Immunity* **45**, 1205–1218 (2016).
11. K. V. Chow, R. M. Sutherland, Y. Zhan, A. M. Lew, Heterogeneity, functional specialization and differentiation of monocyte-derived dendritic cells. *Immunol. Cell Biol.* **95**, 244–251 (2017).
12. A. T. Satpathy *et al.*, Zbtb46 expression distinguishes classical dendritic cells and their committed progenitors from other immune lineages. *J. Exp. Med.* **209**, 1135–1152 (2012).
13. M. M. Meredith *et al.*, Expression of the zinc finger transcription factor zDC (Zbtb46, Btbd4) defines the classical dendritic cell lineage. *J. Exp. Med.* **209**, 1153–1165 (2012).
14. B. U. Schraml *et al.*, Genetic tracing via DNGR-1 expression history defines dendritic cells as a hematopoietic lineage. *Cell* **154**, 843–858 (2013).
15. C. G. Briseño *et al.*, Distinct transcriptional programs control cross-priming in classical and monocyte-derived dendritic cells. *Cell Rep.* **15**, 2462–2474 (2016).
16. N. Anandasabapathy *et al.*, Classical Flt3L-dependent dendritic cells control immunity to protein vaccine. *J. Exp. Med.* **211**, 1875–1891 (2014).
17. S. A. Mollah *et al.*, Flt3L dependence helps define an uncharacterized subset of murine cutaneous dendritic cells. *J. Invest. Dermatol.* **134**, 1265–1275 (2014).
18. J. Helft *et al.*, GM-CSF mouse bone marrow cultures comprise a heterogeneous population of CD11c(+)MHCII(+) macrophages and dendritic cells. *Immunity* **42**, 1197–1211 (2015).
19. A. Lehtonen *et al.*, Gene expression profiling during differentiation of human monocytes to macrophages or dendritic cells. *J. Leukoc. Biol.* **82**, 710–720 (2007).
20. B. Vander Lugt *et al.*, Transcriptional programming of dendritic cells for enhanced MHC class II antigen presentation. *Nat. Immunol.* **15**, 161–167 (2014).
21. M. A. Pearen, G. E. O. Muscat, Minireview: Nuclear hormone receptor 4A signaling: Implications for metabolic disease. *Mol. Endocrinol.* **24**, 1891–1903 (2010).
22. S. E. Mullican *et al.*, Abrogation of nuclear receptors Nr4a3 and Nr4a1 leads to development of acute myeloid leukemia. *Nat. Med.* **13**, 730–735 (2007).
23. R. N. Hanna *et al.*, The transcription factor NR4A1 (Nur77) controls bone marrow differentiation and the survival of Ly6C- monocytes. *Nat. Immunol.* **12**, 778–785 (2011).
24. I. Shaked *et al.*, Transcription factor Nr4a1 couples sympathetic and inflammatory cues in CNS-recruited macrophages to limit neuroinflammation. *Nat. Immunol.* **16**, 1228–1234 (2015).
25. K. Park *et al.*, The transcription factor NR4A3 controls CD103+ dendritic cell migration. *J. Clin. Invest.* **126**, 4603–4615 (2016).
26. S. H. Naik *et al.*, Cutting edge: Generation of splenic CD8+ and CD8- dendritic cell equivalents in Fms-like tyrosine kinase 3 ligand bone marrow cultures. *J. Immunol.* **174**, 6592–6597 (2005).
27. N. Onai *et al.*, Identification of clonogenic common Flt3+M-CSFR+ plasmacytoid and conventional dendritic cell progenitors in mouse bone marrow. *Nat. Immunol.* **8**, 1207–1216 (2007).
28. M. E. Kirkling *et al.*, Notch signaling facilitates in vitro generation of cross-presenting classical dendritic cells. *Cell Rep.* **23**, 3658–3672.e6 (2018).
29. E. L. Gautier *et al.*; Immunological Genome Consortium, Gene-expression profiles and transcriptional regulatory pathways that underlie the identity and diversity of mouse tissue macrophages. *Nat. Immunol.* **13**, 1118–1128 (2012).
30. J. C. Miller *et al.*; Immunological Genome Consortium, Deciphering the transcriptional network of the dendritic cell lineage. *Nat. Immunol.* **13**, 888–899 (2012).
31. M. Guilliams *et al.*, Unsupervised high-dimensional analysis aligns dendritic cells across tissues and species. *Immunity* **45**, 669–684 (2016).
32. K.-W. Kim *et al.*, MHC II+ resident peritoneal and pleural macrophages rely on IRF4 for development from circulating monocytes. *J. Exp. Med.* **213**, 1951–1959 (2016).
33. N. V. Serbina, T. P. Salazar-Mather, C. A. Biron, W. A. Kuziel, E. G. Pamer, TNF/iNOS-producing dendritic cells mediate innate immune defense against bacterial infection. *Immunity* **19**, 59–70 (2003).
34. M. Neuenhahn *et al.*, CD8alpha+ dendritic cells are required for efficient entry of Listeria monocytogenes into the spleen. *Immunity* **25**, 619–630 (2006).
35. B. T. Edelson *et al.*, CD8α(+) dendritic cells are an obligate cellular entry point for productive infection by Listeria monocytogenes. *Immunity* **35**, 236–248 (2011).
36. T. S. P. Heng, M. W. Painter; Immunological Genome Project Consortium, The immunological genome project: Networks of gene expression in immune cells. *Nat. Immunol.* **9**, 1091–1094 (2008).
37. L. Yang, ImmGen microarray phase 1. Gene Expression Omnibus. https://www.ncbi.nlm.nih.gov/geo/query/acc.cgi?acc=GSE15907. Accessed 27 June 2019.
38. C. G. Briseno, Distinct transcriptional programs control cross-presentation in classical- and monocyte-derived dendritic cells. Gene Expression Omnibus. https://www.ncbi.nlm.nih.gov/geo/query/acc.cgi?acc=GSE75015. Accessed 27 June 2019.
39. E. Glasmacher *et al.*, A genomic regulatory element that directs assembly and function of immune-specific AP-1-IRF complexes. *Science* **338**, 975–980 (2012).
40. X. Wu *et al.*, Mafb lineage tracing to distinguish macrophages from other immune lineages reveals dual identity of Langerhans cells. *J. Exp. Med.* **213**, 2553–2565 (2016).
41. H. J. McKenna *et al.*, Mice lacking flt3 ligand have deficient hematopoiesis affecting hematopoietic progenitor cells, dendritic cells, and natural killer cells. *Blood* **95**, 3489–3497 (2000).
42. A. Mildner *et al.*, Genomic characterization of murine monocytes reveals C/EBPβ transcription factor dependence of Ly6C^{-} cells. *Immunity* **46**, 849–862.e7 (2017).
43. S. Suzuki *et al.*, Critical roles of interferon regulatory factor 4 in CD11bhighCD8alpha- dendritic cell development. *Proc. Natl. Acad. Sci. U.S.A.* **101**, 8981–8986 (2004).
44. S. Bajaña, K. Roach, S. Turner, J. Paul, S. Kovats, IRF4 promotes cutaneous dendritic cell migration to lymph nodes during homeostasis and inflammation. *J. Immunol.* **189**, 3368–3377 (2012).
45. G. J. Randolph, K. Inaba, D. F. Robbiani, R. M. Steinman, W. A. Muller, Differentiation of phagocytic monocytes into lymph node dendritic cells in vivo. *Immunity* **11**, 753–761 (1999).
46. S. Boulet, N. Labrecque, NR4A3 plays a pivotal role in the differentiation of monocyte-derived dendritic cells. Gene Expression Omnibus. https://www.ncbi.nlm.nih.gov/geo/query/acc.cgi?acc=GSE99837. Deposited 8 June 2017.